Isomorphic diffuse glioma is a morphologically and molecularly distinct tumour entity with recurrent gene fusions of *MYBL1* or *MYB* and a benign disease course

Annika K. Wefers[1,2,3], Damian Stichel[1,2], Daniel Schrimpf[1,2], Roland Coras[4], Mélanie Pages[5], Arnault Tauziède-Espariat[5], Pascale Varlet[5], Figen Söylemezoglu[6], Ute Pohl[7,8], José Pimentel[9], Jochen Meyer[1,2], Ekkehard Hewer[10], Anna Japp[11], Ahbi Joshi[12], David E. Reuss[1,2], Annekathrin Reinhardt[1,2], Philipp Sievers[1,2], M. Belén Casalini[1,2], Azadeh Ebrahimi[1,2], Kristin Huang[1,2], Christian Koelsche[1,13], Hu Liang Low[14], Olinda Rebelo[15], Albert J. Becker[11], Ori Staszewski[16], Michel Mittelbronn[17-21], Martin Hasselblatt[22], Jens Schittenhelm[23,24], Edmund Cheesman[25], Ricardo Santos de Oliveira[26], Rosane Gomes Queiroz[27], Elvis Terci Valera[27], Volkmar H. Hans[28,29], Andrey Korshunov[1,2], Adriana Olar[30,31], Keith L. Ligon[32], Stefan M. Pfister[3,33,34], Zane Jaunmuktane[35,36], Sebastian Brandner[35,37], David W. Ellison[38], Thomas S. Jacques[39], Mrinalini Honavar[40], Eleonora Aronica[41], Maria Thom[35], Felix Sahm[1,2,3], Andreas von Deimling[1,2], David T.W. Jones[3,42], Ingmar Blumcke[4], David Capper[43,44]

Affiliations

[1] Department of Neuropathology, Institute of Pathology, University Hospital Heidelberg, Heidelberg, Germany

[2] Clinical Cooperation Unit Neuropathology, German Cancer Consortium (DKTK), German Cancer Research Center (DKFZ), Heidelberg, Germany

[3] Hopp Children's Cancer Center Heidelberg (KiTZ), Heidelberg, Germany.

[4] Department of Neuropathology, University Hospital Erlangen, Erlangen, Germany

[5] Department of Neuropathology, Sainte-Anne Hospital, Descartes University, Paris, France

[6] Hacettepe University Faculty of Medicine, Department of Pathology, Ankara, Turkey

[7] Department of Cellular Pathology, Queen's Hospital BHRUT, Romford, UK

[8] Department of Cellular Pathology, Queen Elizabeth Hospital Birmingham/University Hospitals Birmingham, Birmingham, UK

[9] Laboratory of Neuropathology, Department of Neurosciences and Mental Health, Department of Neurology, Hospital de Santa Maria (CHULN, EPE), Lisbon; Faculdade de Medicina, Universidade de Lisboa, Portugal

[10] Institute of Pathology, University of Bern, Bern, Switzerland

[11] Department of Neuropathology, University of Bonn, Bonn, Germany

[12] Department of Neuropathology, Royal Victoria Infirmary, Newcastle upon Tyne, UK

[13] Department of General Pathology, Institute of Pathology, University Hospital Heidelberg, Heidelberg, Germany

[14] Department of Neurosurgery, Queen's Hospital BHRUT, Romford, UK

[15] Neuropathology Unit, Centro Hospitalar de Universidades de Coimbra, Coimbra, Portugal

[16] Institute of Neuropathology, University of Freiburg, Freiburg, Germany

[17] Edinger Institute, Institute of Neurology, University of Frankfurt am Main, Germany

[18] Luxembourg Centre of Neuropathology (LCNP), Dudelange, Luxembourg

[19] Laboratoire National de Santé (LNS), National Center of Pathology (NCP), Dudelange, Luxembourg

[20] Luxembourg Centre for Systems Biomedicine (LCSB), University of Luxembourg, Luxembourg

[21] NORLUX Neuro-Oncology Laboratory, Luxembourg Institute of Health (LIH), Luxembourg

[22] Institute of Neuropathology, University Hospital Münster, Münster, Germany

[23] Department of Neuropathology, Institute of Pathology and Neuropathology, University Hospital of Tübingen, Tübingen, Germany

[24] Center for CNS Tumours, Comprehensive Cancer Center Tübingen-Stuttgart, University Hospital of Tübingen, Tübingen, Germany

[25] Department of Paediatric Histopathology, Royal Manchester Children's Hospital Manchester, UK

[26] Division of Pediatric Neurosurgery, Department of Surgery and Anatomy, Ribeirão Preto Medical School, University of São Paulo, Brazil

[27] Department of Pediatrics, Ribeirão Preto Medical School, University of São Paulo, Brazil

[28] Abteilung Neuropathologie, Institut für klinische Pathologie, Dietrich-Bonhoeffer-Klinikum, Neubrandenburg, Germany

[29] Institut für Neuropathologie, Evangelisches Klinikum Bethel gGmbH, Bielefeld, Germany

[30] Departments of Pathology and Laboratory Medicine & Neurosurgery, Medical University of South Carolina, Charleston, SC, USA

[31] Hollings Cancer Center, Charleston, SC, USA

[32] Department of Oncologic Pathology, Dana-Farber/Brigham and Women's Cancer Center, Harvard Medical School, Boston, MA, USA

[33] Division of Pediatric Neurooncology, German Cancer Research Center (DKFZ) and German Cancer Consortium (DKTK), Heidelberg, Germany

[34] Department of Pediatric Hematology and Oncology, Heidelberg University Hospital, Heidelberg, Germany

[35] Division of Neuropathology, UCL Institute of Neurology, National Hospital for Neurology and Neurosurgery, London, UK

[36] Department of Clinical and Movement Neurosciences, UCL Institute of Neurology, London, UK

[37] Department of Neurodegenerative Disease, UCL Institute of Neurology, London, UK

[38] Department of Pathology, St. Jude Children's Research Hospital, Memphis, TN, USA

[39] Developmental Biology and Cancer Section, UCL Great Ormond Street Institute of Child Health, London, UK

[40] Department of Pathology, Hospital Pedro Hispano, Matosinhos, Portugal

[41] Amsterdam UMC, University of Amsterdam, Department of (Neuro)Pathology, Amsterdam and Stichting Epilepsie Instellingen Nederland, Heemstede, The Netherlands

[42] Pediatric Glioma Research Group, German Cancer Research Center (DKFZ), Heidelberg, Germany

[43] Charité - Universitätsmedizin Berlin, corporate member of Freie Universität Berlin, Humboldt-Universität zu Berlin, and Berlin Institute of Health, Department of Neuropathology, Berlin, Germany

[44] German Cancer Consortium (DKTK), Partner Site Berlin, German Cancer Research Center (DKFZ), Heidelberg, Germany

Corresponding authors:

Dr. Annika Wefers

annika.wefers@med.uni-heidelberg.de

Prof. Dr. David Capper

david.capper@charite.de

Keywords

Abstract

The "isomorphic subtype of diffuse astrocytoma" was identified histologically in 2004 as a supratentorial, highly differentiated glioma with low cellularity, low proliferation and focal diffuse brain infiltration. Patients typically had seizures since childhood and all were operated on as adults. To define the position of these lesions among brain tumours, we histologically, molecularly and clinically analysed 26 histologically prototypical isomorphic diffuse gliomas. Immunohistochemically, they were GFAP-positive, MAP2- and CD34-negative and nuclear ATRX expression was retained. All 24 cases sequenced were IDH-wildtype. In cluster analyses of DNA-methylation data, isomorphic diffuse gliomas formed a group clearly distinct from other glial/glio-neuronal brain tumours and normal hemispheric tissue. It was most closely related to paediatric *MYB/MYBL1* altered diffuse astrocytomas and angiocentric gliomas. 13/25 (52%) of isomorphic diffuse gliomas had copy number alterations of *MYBL1* or *MYB*. Gene fusions of *MYBL1* or *MYB* with various gene partners were detected in 11/22 (50%). Gene fusions were associated with increased RNA-expression of the respective *MYB*-family gene in 83%. Integrating copy number alterations and RNA sequencing data, 20/26 (77%) had either *MYBL1* (54%) or *MYB* (23%) alterations. Clinically, 89% of patients were seizure free after surgery and all had a good outcome. In summary, we here define a distinct tumour class with a concise morphology, a typical DNA-methylation profile and frequent *MYBL1* and *MYB* alterations. It occurs both in children and adults and has a benign disease course. For classification, we propose the term "isomorphic diffuse glioma, *MYBL1/MYB* altered, WHO grade I". DNA-methylation profiling is well suited to identify these tumours.

Introduction

Genome-wide DNA-methylation profiling and identification of recurrent genomic alterations have become important tools for both the molecular classification of known brain tumour entities and the detection of novel entities and subclasses of brain tumours [e.g. 21,50,51,35,28,59,41,7,44,15,23]. One enigmatic glioma entity that has not yet been molecularly characterized in detail is the "isomorphic subtype of diffuse astrocytoma". It was first proposed as a separate entity in 2004 as a supratentorial, epilepsy-associated, highly differentiated, microscopically diffuse glial tumour with low cellularity and low proliferation [3,47]. While all patients in the original description were adults at operation (median age 32 years), most had a history of epileptic seizures since childhood. On cMRI, the tumours displayed a mass effect, a homogenous signal increase on FLAIR and T2-weighted images

and a signal decrease on T1-weighted images. Contrast enhancement was not observed [3,2,55]. Lacking additional evidence of a truly distinct entity, these isomorphic diffuse gliomas have not yet been incorporated into the WHO classification of brain tumours [32]. Using the histological criteria described in 2004, they are rare even among epilepsy associated tumours, accounting for approximately 0.8% to 1.9% in such a setting [4,2]. In a more recent analysis of the same tumours, then termed "isomorphic neuroepithelial tumours" (INET), all isomorphic diffuse gliomas were IDH1 R132H-negative, suggesting that they differ from diffuse astrocytoma, IDH-mutant [2]. In accordance with this, isomorphic diffuse gliomas had a generally benign clinical course without malignant progression [3,47].

In particular when occurring in adults, isomorphic diffuse gliomas may be very problematic to classify. According to the current WHO classification, they fall into the provisional category of diffuse astrocytoma, IDH-wildtype. This category mostly consists of misclassified high-grade gliomas, in particular IDH-wildtype glioblastomas, and a few IDH-wildtype low-grade gliomas [42,5]. Thus, a further characterization and definition of isomorphic diffuse gliomas is required to allow a reliable identification.

Some recurrent genomic alterations in glioma subgroups and glio-neuronal tumours are well established such as IDH-mutations [18,58] and *BRAF*-mutations and -fusions [46,26]. In addition, especially for paediatric low-grade gliomas novel genomic alterations have been detected in recent years. These include gene fusions of *FGFR1–3*, *NTRK2, PRKCA* and *MYB*/*MYBL1* with different fusion partners, or different rearrangements and mutations of these genes [59,37,39,24,54,25,20]. To analyse whether the "isomorphic subtype of diffuse astrocytoma" is a separate tumour entity with distinct molecular alterations, we performed genome-wide DNA-methylation profiling and copy number analyses from FFPE-samples of 26 histologically typical isomorphic diffuse gliomas and, from a subset, *IDH1/2* sequencing and RNA sequencing. Moreover, clinical data of these tumours were evaluated and compared to those of other low-grade glioma entities.

Materials and Methods

Tissue samples, clinical data and reference dataset

Most study cases were diagnosed histologically by members of the International League against Epilepsy (ILAE) brain tumour study group and associated partners since the entity proposal in 2004. Others were obtained from further collaborating institutions (Institute of Pathology, University of Bern, Switzerland; Department of Neuropathology, Sainte-Anne Hospital, Paris, France; Department of Neuropathology, Tübingen, Germany). Formalin-fixed and paraffin-embedded (FFPE) tissue and clinical data were collected at the Department of Neuropathology of the University Hospital Heidelberg (Heidelberg, Germany). Tissue collection and processing and data collection were in accordance with local ethical approvals.

Histology and immunohistochemistry

For all cases, in addition to the histological review at the local centres, a review of an H&E-staining was done by two experienced neuropathologists (DC, AW). For all cases with sufficient material, immunohistochemical staining was performed on a Ventana BenchMark Ultra Immunostainer using either the OptiView DAB IHC Detection Kit or the ultraView

Universal DAB Detection Kit (Ventana Medical Systems, Tucson, Arizona, USA). Antibodies were directed against: Alpha Thalassemia/Mental Retardation Syndrome X-Linked- (ATRX) protein (BSB3296, 1:2000, pretreatment using CC1-buffer, OptiView; BioSB, Santa Barbara, CA, USA), CD34 (Ventana Kit 790-2927, pretreatment CC1, OptiView; Ventana Medical Systems), glial fibrillary acid protein (GFAP; Agilent Dako Z0334, 1:1000, no pretreatment, ultraView; Agilent Technologies, Inc., Santa Clara, CA, USA), microtubule-associated protein 2 (MAP2; Sigma-Aldrich M4403, 1:15000, pretreatment CC1, ultraView; Merck KGaA, Darmstadt, Germany), Ki67 (Agilent Dako M7240, 1:100, pretreatment CC1, OptiView; Agilent), p53 (Novocastra NCL-p53-DO1, 1:50, pretreatment CC1, ultraView; Leica Biosystems, Nussloch, Germany), and IDH1 R132H (internal clone H14 [9], 1:2, pretreatment CC2, ultraView; exemplary stainings only). Stained slides were scanned on a NanoZoomer Digital Slide Scanner (Hamamatsu, Japan) or an Aperio AT2 Scanner (Aperio Technologies, Vista, California, USA) and photographed using Aperio ImageScope software v12.3.2.8013.

DNA and RNA extraction

DNA and, if sufficient tissue was available, RNA were extracted from FFPE tissue of representative tumour areas with the highest tumour cell content. An automated extraction was done with a Maxwell system (Promega, Fitchburg, WI, USA) and the Maxwell 16 FFPE Plus LEV DNA Purification Kit or the Maxwell 16 LEV RNA FFPE Kit according to the manufacturer's instructions. The DNA concentrations were determined with the Invitrogen Qubit dsDNA BR Assay Kit (Thermo Fisher Scientific, Waltham, MA, USA) and a FLUOstar Omega Microplate Reader (BMG Labtech GmbH, Ortenberg, Germany). RNA concentrations and quality were assessed using the Agilent RNA 6000 Nano Assay and an Agilent Bioanalyser 2100 (Agilent Technologies) following the protocols provided by the manufacturer.

IDH sequencing

Targeted sanger sequencing of *IDH1* and *IDH2* was done with 20 ng of DNA as previously described [18] using the following primers: *IDH1* forward 5′-TGATGAGAAGAGGGTTGAGGA-3′, reverse 5′-GCAAAATCACATTATTGCCAAC-3′; *IDH2* forward 5′-GCTGCAGTGGGACCACTATT-3′, reverse 5′-CTCCACCCTGGCCTACCT-3'. Sequences were determined using an ABI 3500 Genetic Analyzer (Applied Biosystems, Foster City, CA, USA) and the Sequence Pilot version 3.1 software (JSI Medical systems GmbH, Ettenheim, Germany).

DNA-methylation profiling

DNA-methylation profiling of all samples was performed with 200–500 ng of DNA using the Infinium HumanMethylation450 BeadChip array (450k) or the Infinium MethylationEPIC BeadChip array (850k; Illumina, Inc., San Diego, CA, USA) at the Genomics and Proteomics Core Facility of the German Cancer Research Center (DKFZ) according to the protocols

provided by the manufacturer. Filtering was performed as previously described [7], and genome-wide copy number analyses were done using the conumee package in R [22].

Copy number alterations of genomic segments were inferred from the methylation array data based on the R-package conumee [22] after additional baseline correction (https://github.com/dstichel/conumee) with a cutoff of 0.1 for gains and −0.1 for losses on log2-scale. Summary copy number profiles were created by summarizing these data from the samples. The status of both the *MYBL1-* and *MYB*-loci and neighbouring regions within 2 Mb from *MYBL1* and *MYB* was determined by evaluating the respective probes according to the IlluminaHumanMethylation450kmanifest [16] or IlluminaHumanMethylationEPICmanifest [17], respectively. Results were verified manually using the Integrative Genomics Viewer [43] to exclude a misinterpretation in single cases with high background noise or very focal alterations.

Reference cases for an unsupervised hierarchical cluster analysis and a t-SNE-analysis included well-characterized cases belonging to the following methylation classes [7 and www.molecularneuropathology.org/mnp/classifier/2]: hemispheric cortex (n = 9); white matter (n = 9); low grade glioma, dysembryoplastic neuroepithelial tumour (n = 13); low grade glioma, ganglioglioma (n = 15); low grade glioma, subclass hemispheric pilocytic astrocytoma and ganglioglioma (n = 10); low grade glioma, subclass midline pilocytic astrocytoma (n = 15); low grade glioma, subclass posterior fossa pilocytic astrocytoma (n = 11); (anaplastic) pleomorphic xanthoastrocytoma (n = 15); anaplastic astrocytoma with piloid features [41] (n = 15); diffuse midline glioma H3 K27M mutant (n = 14); glioblastoma, IDH wildtype, H3.3 G34 mutant (n = 10); glioblastoma, IDH wildtype, subclass mesenchymal (n = 15); glioblastoma, IDH wildtype, subclass midline (n = 10); glioblastoma, IDH wildtype, subclass RTK I (n = 15); glioblastoma, IDH wildtype, subclass RTK II (n = 8). Moreover, as isomorphic diffuse gliomas have in the past often been diagnosed as diffuse astrocytoma, WHO grade II, cases with the integrated diagnosis of diffuse astrocytoma, IDH-mutant, WHO grade II (n = 8) were selected for comparison. In addition, tumours with the integrated diagnosis of angiocentric glioma, i.e. tumours with a histology compatible with this diagnosis, a methylation profile typical of angiocentric glioma and proven *MYB-QKI* fusions in all cases with sufficient RNA for RNA sequencing, were included in the analyses (n = 15). This was done because we noticed that both angiocentric gliomas and isomorphic diffuse gliomas are classified as methylation class low-grade glioma, *MYB/MYBL1* with the recently published brain tumour classifier [7]. The test cases were further compared to published DNA-methylation data from seven paediatric *MYB/MYBL1* altered diffuse astrocytomas [37].

RNA sequencing and RT-PCR

RNA sequencing of samples for which RNA of sufficient quality and quantity was available (n = 22) was performed on a NextSeq 500 (Illumina) as described previously [45,49]. Fusion detection was done using Arriba (https://github.com/suhrig/arriba/). Fusions of the *MYBL1-* and *MYB*-genes were verified by RT-PCR. cDNA was generated using TruSeq RNA Access (Illumina, Inc., San Diego, CA, USA). Primer sequences are available upon request. For one case in which a *MAML2-MYBL1* fusion was detected by RNA sequencing from FFPE-tissue, the inverse *MYBL1-MAML2* fusion was verified by RT-PCR from fresh frozen tissue of the same tumour (#12).

Expected counts of *MYBL1* and *MYB* expression were calculated using rsem [29]. RNA sequencing data from pilocytic astrocytomas (n = 5) were used for comparison. *MYBL1* expression of individual *MYBL1* altered isomorphic diffuse gliomas was regarded as increased if it exceeded the expression of that of all pilocytic astrocytomas and that of all *MYB* altered isomorphic diffuse gliomas. *MYB* expression of individual *MYB* altered isomorphic diffuse gliomas was regarded as increased if it exceeded the expression of that of all pilocytic astrocytomas and that of all *MYBL1* altered isomorphic diffuse gliomas.

Statistics

For an unsupervised hierarchical cluster analysis of isomorphic diffuse gliomas and reference classes, we selected the 10,000 most variably methylated CpG sites across the dataset according to median absolute deviation. Clustering was done using the Euclidean distance and Ward linkage. For unsupervised 2D representation of pairwise sample correlations, dimensionality reduction by t-distributed stochastic neighbor embedding (t-SNE) was done with the R-package Rtsne (https://github.com/jkrijthe/Rtsne) using the 10,000 most variable CpG sites according to the standard deviation, 1000 iterations and a perplexity value of 10.
RNA-expression data were compared with a Kruskal-Wallis test followed by post hoc Dunn's multiple comparisons test using Prism 8.02 (GraphPad, La Jolla, CA, USA). p-values of less than 0.05 were considered significant.
Overall survival of 18 patients with isomorphic diffuse glioma was compared to that of patients with pilocytic astrocytoma WHO grade I (n = 82), angiocentric gliomas WHO grade I (n = 10) and diffuse astrocytoma, IDH-mutant, WHO grade II (n = 181). Survival data were analysed by Kaplan-Meier analysis and compared using the log-rank test with Prism.

Results

Isomorphic diffuse gliomas are monomorphic IDH-wildtype gliomas with moderately increased cell density

As a first step, we histologically identified tumours in accordance with the criteria specified for the "isomorphic subtype of diffuse astrocytomas" or "isomorphic neuroepithelial tumour" [3,2]. These cases were mainly diagnosed by members of the ILAE brain tumour study group and associated partners since the proposal of the entity in 2004. One case of the original series [3] was available for further analyses in this study (our case #19). The other 25 cases represent newly identified specimens. Histologically, the tumours shared a low to moderate increase in cellular density in an often slightly pronounced neurofibrillary matrix (Fig. 1a–e). The tumour cells typically had monomorphic, round nuclei with finely dispersed chromatin and inconspicuous nucleoli (insets in Fig. 1a–d). Occasionally, the nuclei were very small and chromatin-dense, which may be a result of fixation conditions (Fig. 1e). In many cases, the neurofibrillary matrix showed some degree of microcystic changes (Fig. 1 c, d, e). In these areas, the tumour cell bodies could be distinguished and frequently had many fine glial processes (inset Fig. 1d). One tumour focally showed myxoid changes of the tumour matrix with interspersed neurons, resembling the glio-neuronal element of dysembryoplastic

neuroepithelial tumours (DNT; Fig. 1f), while other areas showed a typical isomorphic morphology.

In some of the cases, it was challenging to differentiate between tumour and normal white matter. In 23/26 tumours, the tumour cells microscopically diffusely infiltrated the adjacent brain structures such as the neocortex. Thus, scattered residual neurons were visible in most of the isomorphic diffuse gliomas (arrows in Fig. 1 b, e, f).

Immunohistochemistry was done on 19 cases. The tumour cells of all cases were embedded in a glial fibrillary acid protein (GFAP) positive matrix (Fig. 1g) and seemed to express this protein. In all cases, the tumour cells were negative for microtubule-associated protein 2 (MAP2), whereas residual neurons or neuronal processes between the tumour cells were frequently positive (Fig. 1h). The tumour cells were also CD34 negative with only blood vessels staining positive (Fig. 1i). *IDH1/2*-wildtype status was verified by Sanger sequencing of 24 cases with sufficient DNA. An exemplary IDH1 R132H staining is shown in Figure 1j. The Alpha Thalassemia/Mental Retardation Syndrome X-Linked- (ATRX) protein was retained in the tumour cell nuclei in all cases (Fig. 1k). Proliferation was below 1% in all cases analysed (Fig. 1l) and mitoses were not identified. A prominent accumulation of the p53-protein was never observed (data not shown). The vasculature was inconspicuous. Necrosis was not observed.

Isomorphic diffuse glioma is a distinct molecular tumour entity defined by a specific DNA-methylation profile

We have previously demonstrated that DNA-methylation profiling is a powerful tool to molecularly define clinico-pathological brain tumour entities [6,41,48,12,50,35,7]. Thus, we performed a genome wide DNA-methylation analysis of all 26 isomorphic diffuse gliomas. Both in an unsupervised hierarchical cluster analysis and in a t-distributed stochastic neighbor embedding (t-SNE) analysis together with 246 cases from 17 reference methylation classes of glial/glio-neuronal tumours plus normal white matter and cortex, isomorphic diffuse gliomas consistently formed a distinct cluster (Fig. 2a, b). The cluster was clearly separate from all other reference cases including diffuse astrocytoma, IDH-mutant, low-grade IDH-wildtype glio-neuronal tumours such as DNT and ganglioglioma, but also white matter and cortex. Also, it did not show any resemblance to IDH-wildtype high-grade glioma methylation classes. The closest relation was found to the cluster of angiocentric gliomas. These data indicate that isomorphic diffuse glioma is a distinct molecular entity with a DNA-methylation profile closely related to angiocentric glioma.

Isomorphic diffuse gliomas have frequent copy number alterations of *MYBL1* and *MYB*

We next analysed copy number variation profiles (CNP) calculated from the methylation array data (n = 25 evaluable; in case #14 the background noise was too high to allow an analysis). The copy number profiles analysed showed only few copy number alterations. However, the analysis revealed that 10/25 tumours (40%) had focal copy number alterations affecting the *MYBL1*-locus (6q23.3; Fig. 3a, b, Supplementary Fig. 1) and 3/25 (12%) showed copy number alterations of the *MYB*-locus (8q13.1; Fig. 3c, d, Supplementary Fig. 1). For *MYBL1*, the alterations included focal gains (n = 5, Fig. 3a), losses (n = 4, Fig. 3b) and

complex rearrangements of chromosome 8 (n = 1). Of the tumours with rearrangements of the *MYB*-locus, one tumour had a *MYB*-gain (Fig. 3c), one had a *MYB*-loss (Fig. 3d) and one tumour showed losses in distances of approximately 750 kb 5' and 460 kb 3' of the *MYB*-locus, likely indicating a rearrangement of the *MYB*-locus. One additional tumour showed both a loss of the *MYB*-locus on 6q and a gain of the *MYBL1*-locus on 8q which possibly represents artefacts.

Of all cases with CNP alterations of *MYBL1* or *MYB*, eleven cases (85%) had broader gains/losses of *MYBL1* or *MYB* and adjacent loci which were evident from a low resolution copy number profile. Two tumours (15%) had small gains/losses identifiable only when the copy number profiles were investigated in detail using the integrated genomic viewer [43].

Of the remaining copy number profiles without *MYBL1*/*MYB* copy number alterations, six had changes on chromosomes 6 or 8 which did not indicate a specific *MYBL1*/*MYB* alteration. Of these, one copy number profile showed a gain at the 3' end of 6p. Five copy number profiles indicated a gain at the 5' end of 8p which however was also occasionally seen in different tumour entities and thus may represent an artefact. Finally, another tumour had changes which were neither on chromosome 6 nor 8 while the copy number profiles of four cases were balanced. Altogether, we detected alterations of the *MYBL1*- or *MYB*-loci in 13/25 (52%) of the isomorphic diffuse gliomas analysed (Supplementary Fig. 1; Table 1, Supplementary Table 1).

MYBL1 or *MYB* gene fusions and corresponding RNA overexpression are frequent in isomorphic diffuse gliomas

The focal structural alterations described above may indicate the presence of gene fusions. To confirm such fusions, we performed RNA sequencing of all cases with sufficient material (n = 22). *MYBL1* fusions were detected in 8/22 tumours (36%; Fig. 4a). The only recurrent fusion partner of *MYBL1* was *MMP16* in 2/22 tumours (9%; Fig. 4a). Further fusion partners of *MYBL1*, validated by RT-PCR, were *RAD51B, MAML2, ZFHX4* and *TOX* as well as intergenic sites on chromosomes 8 and 10 (n = 1 each). In all detected fusion genes, *MYBL1* was truncated after exon 8, 9 or 10, resulting in a loss of the negative regulatory C-myb domain [53,14] (Fig. 4a).

In an additional case, RNA sequencing indicated that the region 5' of *MYBL1* was fused to MMP16 (not shown). Together with a *MYBL1*-gain in the copy number profile, this may indicate a complex rearrangement involving the *MYBL1*-locus that was not fully resolvable with the techniques used, e.g. resulting in an enhancer hijacking or alternative transcription start site.

Some fusions were associated with corresponding changes of the copy number profile: The *MYBL1-MMP16* fused cases showed corresponding duplications in the copy number profile (Fig. 3a) while the *MYBL1-TOX* fusion was associated with a focal loss of 8q between *MYBL1* and *TOX* (Fig. 3b).

MYB fusions were detected in 3/22 (14%) cases (Fig. 4b). Two cases with balanced copy number profile had *MYB-PCDHGA1* fusions. In a case with a *MYB*-gain (Fig. 3c), we detected two *MYB-HMG20A* fusions with two different breakpoints in *MYB*. In addition to the gain of *MYB*, also a gain of *HMG20A* on 15q was visible in the CNP of this case (Fig. 3c) While some of the fusions resulted in a truncation of *MYB* before the negative regulatory C-

myb domain reminiscent of the *MYBL1* fusions, others resulted in a truncation downstream of the C-myb domain leading to a loss of the 3' miRNA-binding sites of *MYB*. This has also been shown to lead to an activation of *MYB* [10,57,60].

In summary, we detected *MYBL1* or *MYB* fusions in 11/22 (50%) of the cases analysed by RNA sequencing (Fig. 4e; Table 1, Supplementary Table 1). In an additional case, the breakpoint detected was 5' of *MYBL1* while the copy number profile suggests that *MYBL1* may also be involved.

Deletion of the C-terminal regions of *MYBL1* or *MYB* has been shown to result in an upregulation of the corresponding gene [1,36]. We therefore quantified the *MYBL1* and *MYB* expression from the RNA sequencing data. Quantification of the mRNA-expression of *MYBL1* confirmed an increased *MYBL1* expression in tumours with corresponding alterations in the CNP and/or RNA sequencing ("*MYBL1* IDG"; n = 13) as compared to pilocytic astrocytomas ("PA"; n = 5; adjusted p = 0.022; Fig. 4c). There was a trend of an increased *MYBL1* expression in *MYBL1* altered isomorphic diffuse gliomas compared to isomorphic diffuse gliomas without detected *MYBL1*/*MYB* alteration ("other IDG" ; n = 5; p = 0.06). Expression in *MYBL1* IDG did not significantly differ from that in *MYB* altered isomorphic diffuse gliomas ("*MYB* IDG"; n = 4), possibly due to the small sample size of the latter (p = 0.32; PA vs. *MYB* IDG; PA vs. other IDG and *MYB* IDG vs. other IDG p > 0.99). The isomorphic diffuse glioma with a rearrangement with breakpoint 5' of *MYBL1* (#3) also had an increased *MYBL1* expression. Of the isomorphic diffuse gliomas without detected *MYBL1*/*MYB* alteration, one case showed a clearly increased *MYBL1* expression, possibly indicating an undetected rearrangement of *MYBL1* or some other process resulting in *MYBL1* induction.

Isomorphic diffuse gliomas with a *MYB* alteration in the CNP and/or RNA sequencing (n = 4) showed a higher expression of *MYB* than *MYBL1* IDG (adjusted p = 0.009; Fig. 4d). Expression between the other groups did not differ (PA vs. *MYBL1* IDG p = 0.51; *MYB* IDG vs. other IDG p = 0.47; PA vs. *MYBL1* IDG, PA vs. other IDG and *MYBL1* IDG vs. other IDG p > 0.99). One case in the group of isomorphic diffuse gliomas without detected *MYBL1*/*MYB* alteration showed an increased *MYB* expression, even higher than that of the other *MYB* altered tumours. This possibly indicates an undetected rearrangement of *MYB* or some other process resulting in *MYB* induction.

Altogether, 14/22 of isomorphic diffuse gliomas (64%) showed an increased expression of *MYBL1* or *MYB*.

In summary of all findings, our data indicates that at least 77% of isomorphic diffuse gliomas have alterations of *MYBL1* or *MYB* (n = 20/26, 77%; Fig. 4e; Table 1, Supplementary Table 1). For three cases for which we did not detect copy number alterations of *MYBL1* or *MYB*, RNA sequencing data are not available. It is possible that these cases have fusions of a *MYB*-family gene that are not evident from the copy number profile. Thus, the percentage of *MYBL1*/*MYB* altered isomorphic diffuse gliomas may be even higher.

Isomorphic diffuse gliomas are related to paediatric *MYB*/*MYBL1* altered diffuse astrocytomas

To see how the isomorphic diffuse gliomas in our cohort relate to paediatric *MYB*/*MYBL1* altered diffuse astrocytomas, we did an additional unsupervised hierarchical cluster analysis

of the cases contained in Fig. 2 with published methylation data from seven paediatric *MYB*/*MYBL1* altered diffuse astrocytomas [37]. Of note, while these paediatric cases were related to the isomorphic diffuse gliomas, they still formed a cluster clearly distinct from all but two paediatric isomorphic diffuse gliomas (Supplementary Fig. 2a). This does not seem to be an effect sole related to the age of the patients at operation, as 4/6 (67%) paediatric isomorphic diffuse gliomas clearly mixed with their adult counterparts in the separate cluster exclusively containing isomorphic diffuse gliomas (Supplementary Fig. 2a). Also, in a t-SNE analysis of the same cases (Supplementary Fig. 2b), most paediatric *MYB*/*MYBL1* altered diffuse astrocytomas separated from isomorphic diffuse glioma with the identical two isomorphic diffuse gliomas falling in close proximity. In addition, two paediatric *MYB*/*MYBL1* altered diffuse astrocytomas intermingled with the neighbouring isomorphic diffuse gliomas. Thus, while the majority of isomorphic diffuse gliomas clearly separated from the paediatric *MYB*/*MYBL1* altered diffuse astrocytomas with these analyses, the data indicate a close relation of these two groups, probably with partial overlap. An analysis of a larger number of cases will be needed to define the whole spectrum of *MYB*/*MYBL1* altered gliomas.

Isomorphic diffuse gliomas are epilepsy-associated tumours with a good prognosis

Analysis of clinical data demonstrated that in our series of 26 cases, eight patients were female and 18 male (approaching a significant difference; p=0.08, binomial test). All tumours were supratentorial and almost half of the tumours had a temporal localisation (n = 11/26; 42%). Twenty-four of 26 patients (92%) had epileptic seizures. The median age at onset of epilepsy was 10 ± 6 years (range 1–35 years; n = 19). In 17/21 patients (81%), epilepsy started during childhood and 6/26 patients (23%) were operated on as children (median age for these cases 8 ± 3 years, range 4–12 years). However, the overall median age at surgery was 29 ± 14 years (range 4–50 years, n = 26). Median time to operation after onset of epilepsy was 15 ± 12 years (range 1–41 years, n = 18).

The median available follow-up time was 2 ± 5 years after surgery (range 0.3–23 years, n = 18). None of the patients died during follow up. Only one patient initially had a recurrence, but not again after a second surgery. None of the patients were reported to receive additional radio- or chemotherapy. Statistical analysis of the survival data is complicated by the fact that most patients were lost to follow up relatively shortly after resection. Not surprisingly, no statistical difference was observed compared to the WHO grade I tumours angiocentric glioma and pilocytic astrocytoma (Fig. 5). Outcome appeared better when compared to a series of diffuse astrocytomas, IDH-mutant, WHO grade II though this was, probably due to sample size and short follow-up, not statistically significant (p = 0.127; Fig. 5).

Of 18 patients with epileptic seizures for whom follow-up data was available, 16 (89%) were permanently seizure-free after surgery and the other two had a reduction in seizure frequency. Thus, it is very likely that the seizures were tumour related. Many patients had had seizures for decades before surgery. We therefore calculated the survival after onset of epilepsy. The median time after onset of epilepsy until patients were lost to follow-up after surgery was 17 ± 13 years (range 2–42 years, n = 18; all patients alive). This also indicates a benign course of these tumours.

Discussion

In this study, we demonstrate that isomorphic diffuse glioma is a tumour class that is molecularly distinct from other established glial/glio-neuronal tumour entities. We show that isomorphic diffuse glioma is IDH-wildtype and should be in the differential diagnoses of low-grade epilepsy-associated tumours in both children and adults. Recognizing these tumours is important as according to the current WHO classification, tumours with the characteristics of isomorphic diffuse gliomas may be misleadingly categorized as diffuse astrocytoma, IDH-wildtype [32], an inhomogeneous group that, particularly in adults, includes a high number of glioblastomas [42].

Due to our histologically defined entry criteria, all tumours analysed in this study shared an isomorphic phenotype with round nuclei and moderate cell density (Fig. 1) as described before [3]. Compared to diffuse astrocytomas, IDH-mutant, WHO grade II the morphology was much more monomorphic. In addition, the Ki67 proliferation index was below 1% in the cases of this series (Fig. 1l). The tumours microscopically showed a focal diffuse growth into pre-existing brain, with scattered residual neurons frequently entrapped within the tumours. This microscopically diffuse growth contrasts with the MRI images of isomorphic diffuse gliomas in which they have been described to be well circumscribed [3]. Thus, while IDH-mutant gliomas diffusely infiltrate the whole brain and tumour cells can immunohistochemically be detected in areas remote from the tumour bulk [8], isomorphic diffuse gliomas likely only locally show a diffuse growth pattern which may explain the excellent prognosis after surgery alone. It is thus important to realize that local diffuse growth does not *per se* indicate an extensive spread of the tumour or a malignant clinical course.

As isomorphic diffuse glioma is a rare entity, many pathologists will only infrequently encounter such a tumour and a diagnosis based on histology alone may be challenging. Still, in our series, in most cases the histology clearly differed from other glial/glioneuronal tumours. While the nuclei of the tumour cells were occasionally more condensed and smaller, resembling oligodendrocytes or oligodendrocyte-like nuclei of DNT, only one single tumour focally contained a small area resembling the glio-neuronal element of DNT (Fig. 1f). In the remaining areas of this tumour, the cells showed the typical isomorphic diffuse growth pattern and the methylation profile of these two morphologically different areas was similar (not shown).

Though sometimes the scattered residual neurons in isomorphic diffuse glioma may have an unusual morphology, isomorphic diffuse glioma histologically separates from ganglioglioma as it does not contain clearly dysplastic binucleated ganglion cells, typically has a highly isomorphic phenotype and is CD34-negative.

Further, the morphology is more isomorphic than what is usually encountered in infiltration zones of IDH-wildtype glioblastomas and the proliferation was exceedingly low. However, due to the low cell density, some isomorphic diffuse gliomas may be difficult to distinguish from normal white matter, based on histology alone. While a specific immunohistochemical marker is still lacking, 850k DNA-methylation profiling [7] was most helpful for the diagnosis of isomorphic diffuse glioma for these cases.

During the definition of methylation classes of the brain tumour classifier [7], we only had access to relatively few gliomas with *MYB* or *MYBL1* alterations. Thus, in the current version of the classifier (V11b4), only one methylation class of "low-grade glioma, *MYB/MYBL1* altered" is defined. Both isomorphic diffuse gliomas and angiocentric gliomas typically will currently be assigned to this methylation class. By adding more isomorphic diffuse gliomas and thereby increasing the number of cases in this molecular group with this study, we can now demonstrate the presence of subgroups within the methylation class "low-grade glioma, *MYB/MYBL1* altered" as shown by cluster and t-SNE analyses. These subgroups are clearly related to the histological classes of angiocentric glioma and isomorphic diffuse glioma (Fig. 2), showing that there are at least two separate entities within this methylation class. It is possible that inclusion of additional cases will lead to even more subclasses as was recently demonstrated for ependymoma of the methylation class posterior fossa group A [34]. The ongoing refinement of methylation classes will require a continuous adaptation of the brain tumour classifier. For the next update, we are planning to establish two methylation subclasses corresponding to angiocentric glioma and isomorphic diffuse glioma.

MYB or *MYBL1* fusions have been detected in a variety of tumour entities such as adenoid cystic carcinoma [36,19], T-cell acute lymphoblastic leukaemia [31], acute basophilic leukaemia [38], blastic plasmacytoid dendritic cell neoplasm [52] and, in the CNS, angiocentric glioma [1] and paediatric diffuse gliomas/astrocytomas [59,39,37,54,13,1]. *MYB* and *MYBL1* belong to one gene family closely related to *v-MYB*. They are transcription factors that target genes involved in proliferation, survival and differentiation of various tissues [40]. Both proteins have three main protein domains: an N-terminal DNA-binding domain with three MYB binding sites ("Swi3, Ada2, N-Cor, and TFIIIB" - SANT), a central transactivating domain (LMSTEN) and a C-terminal negative regulatory domain (C-myb) [56,33]. In addition, *MYB* has 3' UTR binding sites for several microRNAs which also negatively regulate *MYB* mRNA stability and translation [10,30,11]. *In situ* studies and analyses of different tumours have shown that fusions resulting in a loss of the 3' negative regulatory C-myb domains of *MYB* and *MYBL1*, or the loss of the 3' UTR miRNA binding sites of *MYB*, result in an activation and overexpression of the respective gene [36,27].

The gene fusions defining most cases of angiocentric gliomas are *MYB-QKI* fusions and rarely *MYB-ESR1* fusions [1,59]. In these fusions, *MYB* is truncated at the 3' end, leading to an activation of *MYB* by the removal of negative regulatory domains [1]. We never observed such highly prototypical *MYB-QKI* fusions in isomorphic diffuse gliomas. Instead, we detected various *MYBL1* and *MYB* fusions with different fusion partners. As these fusions also result in a truncation of the C-terminus of *MYBL1* and *MYB* and as we detected high levels of the corresponding mRNAs, the mechanism resulting in tumour growth may be closely related to that of angiocentric glioma. However, as we also detected intergenic sites as fusion partners of *MYBL1,* it seems likely that in isomorphic diffuse gliomas a sole gene fusion inducing overexpression of *MYBL1* or *MYB* is sufficient for tumour development while in angiocentric gliomas the fusion partner, i.e. almost exclusively *QKI*, also plays an important role. It has been demonstrated that apart from *MYB* activation by truncation, the *MYB-QKI* fusions of angiocentric gliomas lead to a hemizygous loss of the tumour suppressor *QKI* [1]. Moreover,

they also involve an enhancer translocation additionally driving aberrant *MYB-QKI* expression [1].

Of note, the presence of either a *MYBL1* or a *MYB* fusion in isomorphic diffuse gliomas with varying fusion partners was not associated with differences in the DNA-methylation profile as we detected cluster trees with mixed alterations (Supplementary Fig. 2a). Thus, although isomorphic diffuse gliomas show a range of alterations involving either *MYBL1* or *MYB* or in a few cases possibly other so far undetected alterations, DNA-methylation analysis indicates that isomorphic diffuse glioma represents a homogenous methylation class.

Several *MYB* and *MYBL1* fusions and rearrangements were recently detected in "paediatric diffuse astrocytomas" [59,39,37,54,1], i.e. paediatric *MYB/MYBL1* altered gliomas other than angiocentric glioma with an astrocytic morphology. The *MYB* and *MYBL1* alterations found in these rare gliomas (n = 12 in total with sequencing data [59,37,39]) included fusions with one gene partner (n = 6/12, 50%), complex fusions with more than one gene partner (n = 1/12, 8%), and *MYBL1* tandem duplications (n = 5/12, 42%). While some gene fusions which we detected in adult isomorphic diffuse gliomas have also been described in paediatric diffuse astrocytomas in the literature, others represent novel fusions. In isomorphic diffuse gliomas *MYBL1* fusions were the most abundant, while fusions in previously published paediatric diffuse astrocytomas primarily affected *MYB*. Importantly, our study clarifies that *MYB/MYBL1* altered gliomas also exist in adults, as to date only paediatric *MYB/MYBL1*-altered diffuse gliomas have been described [59,39,54,37,1]. While there is a close relation between isomorphic diffuse glioma and the published paediatric *MYB/MYBL1*-altered diffuse gliomas, or probably even a partial overlap, cluster analyses indicate that nonetheless isomorphic diffuse glioma is a distinct glioma entity (Supplementary Fig. 2).

We investigated whether specific copy number alterations may predict specific gene fusions in isomorphic diffuse gliomas and thus add diagnostic information. 48% of isomorphic diffuse gliomas showed alterations of the *MYBL1*-locus and 12% of the *MYB*-locus. While a prediction of a certain gene fusion from the copy number alterations was not possible in many cases, a *MYBL1-MMP16* fusion led to a segmental gain on chromosome 8 from *MYBL1* to *MMP16* (Fig. 3a; #1 and 2). In a case with *MYBL1-TOX* fusion (# 5), a deletion between these genes was visible in the copy number profile (Fig. 3b). Also, a *MYB-HMG20A* fusion could retrospectively be deduced from gains of regions both around *MYB* and *HMG20A* (Fig. 3c; # 15). Thus, in some cases, the copy number profile may indicate certain gene fusions. However, RNA sequencing is still needed in cases with balanced copy number profile, for the detection of novel *MYBL1* or *MYB* fusions which do lead to specific copy number alterations but have not been described yet, and for copy number profiles which show alterations of *MYBL1* or *MYB* but do not indicate a specific fusion partner.

How should *MYBL1/MYB* altered isomorphic diffuse gliomas be classified? There is an ongoing debate about the usage of the term "diffuse" when describing a brain tumour. While one interpretation focusses on the extensive spread of tumour cells throughout the brain such as in diffuse glioma, IDH-mutant, another usage refers to the local diffuse growth into adjacent brain structures as seen in isomorphic diffuse gliomas. The second interpretation was implemented in the recent cIMPACT-NOW update 4 on "paediatric-type" diffuse gliomas

which includes *MYB* and *MYBL1* altered diffuse gliomas [13]. Using the term "isomorphic diffuse glioma", we chose to follow this latter proposal. However, while the cIMPACT-NOW update 4 distinguishes between "Diffuse glioma, *MYB*-altered" and "Diffuse glioma, *MYBL1*-altered" regardless of the histology and the DNA-methylation profile, for isomorphic diffuse gliomas we do not see a difference in the DNA-methylation profiles of tumours with different alterations of either *MYB*-family gene. Therefore, we suggest summarizing them as "isomorphic diffuse glioma, *MYBL1/MYB* altered" for classificatory purposes and grade them according to WHO grade I.

In summary, isomorphic diffuse glioma is a morphologically recognizable and molecularly distinct IDH-wildtype glioma with alterations of the *MYBL1*- and less frequently the *MYB*-gene that exists both in paediatric and in adult patients. Isomorphic diffuse glioma has a specific DNA-methylation profile, related to but distinct from that of angiocentric glioma and paediatric *MYB/MYBL1* altered diffuse astrocytomas. It forms a homogenous methylation group, irrespective of different *MYBL1* and *MYB* alterations detected in individual tumours. Thus, DNA-methylation analysis is well suited to help identify these cases and separate them from other glioma entities. Patients with isomorphic diffuse glioma have a good prognosis. For an integrated genotype-phenotype tumour classification, we propose the term "isomorphic diffuse glioma, *MYBL1/MYB* altered, WHO grade I".

Acknowledgements

References

1. Bandopadhayay P, Ramkissoon LA, Jain P, Bergthold G, Wala J, Zeid R, Schumacher SE, Urbanski L, O'Rourke R, Gibson WJ, Pelton K, Ramkissoon SH, Han HJ, Zhu Y, Choudhari N, Silva A, Boucher K, Henn RE, Kang YJ, Knoff D, Paolella BR, Gladden-Young A, Varlet P, Pages M, Horowitz PM et al. (2016) MYB-QKI rearrangements in angiocentric glioma drive tumorigenicity through a tripartite mechanism. Nat Genet 48:273-282. doi:10.1038/ng.3500

2. Blumcke I, Aronica E, Urbach H, Alexopoulos A, Gonzalez-Martinez JA (2014) A neuropathology-based approach to epilepsy surgery in brain tumors and proposal for a new terminology use for long-term epilepsy-associated brain tumors. Acta Neuropathol 128:39-54. doi:10.1007/s00401-014-1288-9

3. Blümcke I, Luyken C, Urbach H, Schramm J, Wiestler O (2004) An isomorphic subtype of long-term epilepsy-associated astrocytomas associated with benign prognosis. Acta Neuropathol 107:381-388. doi:10.1007/s00401-004-0833-3

4. Blumcke I, Spreafico R, Haaker G, Coras R, Kobow K, Bien CG, Pfäfflin M, Elger C, Widman G, Schramm J, Becker A, Braun KP, Leijten F, Baayen JC, Aronica E, Chassoux F, Hamer H, Stefan H, Rössler K, Thom M, Walker MC, Sisodiya SM, Duncan JS, McEvoy AW, Pieper T et al. (2017) Histopathological Findings in Brain Tissue Obtained during Epilepsy Surgery. New Engl J Med 377:1648-1656. doi:10.1056/NEJMoa1703784

5. Brat DJ, Verhaak RG, Aldape KD, Yung WK, Salama SR, Cooper LA, Rheinbay E, Miller CR, Vitucci M, Morozova O, Robertson AG, Noushmehr H, Laird PW, Cherniack AD, Akbani R, Huse JT, Ciriello G, Poisson LM, Barnholtz-Sloan JS, Berger MS, Brennan C, Colen RR, Colman H, Flanders AE, Giannini C et al. (2015) Comprehensive, Integrative Genomic Analysis of Diffuse Lower-Grade Gliomas. N Engl J Med 372:2481-2498. doi:10.1056/NEJMoa1402121

6. Capper D, Engel NW, Stichel D, Lechner M, Glöss S, Schmid S, Koelsche C, Schrimpf D, Niesen J, Wefers AK, Jones DTW, Sill M, Weigert O, Ligon KL, Olar A, Koch A, Forster M, Moran S, Tirado OM, Sáinz-Japeado M, Mora J, Esteller M, Alonso J, del Muro XG, Paulus W et al. (2018) DNA methylation-based reclassification of olfactory neuroblastoma. Acta Neuropathol 136:255-271. doi:10.1007/s00401-018-1854-7

7. Capper D, Jones DTW, Sill M, Hovestadt V, Schrimpf D, Sturm D, Koelsche C, Sahm F, Chavez L, Reuss DE, Kratz A, Wefers AK, Huang K, Pajtler KW, Schweizer L, Stichel D, Olar A, Engel NW, Lindenberg K, Harter PN, Braczynski AK, Plate KH, Dohmen H, Garvalov BK, Coras R et al. (2018) DNA methylation-based classification of central nervous system tumours. Nature 555:469-474. doi:10.1038/nature26000

8. Capper D, Weißert S, Balss J, Habel A, Meyer J, Jäger D, Ackermann U, Tessmer C, Korshunov A, Zentgraf H, Hartmann C, von Deimling A (2010) Characterization of R132H Mutation-specific IDH1 Antibody Binding in Brain Tumors. Brain Pathol 20:245-254. doi:10.1111/j.1750-3639.2009.00352.x

9. Capper D, Zentgraf H, Balss J, Hartmann C, von Deimling A (2009) Monoclonal antibody specific for IDH1 R132H mutation. Acta Neuropathol 118:599-601. doi:10.1007/s00401-009-0595-z

10. Chung EY, Dews M, Cozma D, Yu D, Wentzel EA, Chang T-C, Schelter JM, Cleary MA, Mendell JT, Thomas-Tikhonenko A (2008) c-Myb oncoprotein is an essential target of the dleu2 tumor suppressor microRNA cluster. Cancer Biol Ther 7:1758-1764. doi:10.4161/cbt.7.11.6722

11. Ciceri G, Dehorter N, Sols I, Huang ZJ, Maravall M, Marin O (2013) Lineage-specific laminar organization of cortical GABAergic interneurons. Nat Neurosci 16:1199-1210. doi:10.1038/nn.3485

12. Deng MY, Sill M, Chiang J, Schittenhelm J, Ebinger M, Schuhmann MU, Monoranu C-M, Milde T, Wittmann A, Hartmann C, Sommer C, Paulus W, Gärtner J, Brück W, Rüdiger T, Leipold A, Jaunmuktane Z, Brandner S, Giangaspero F, Nozza P, Mora J, Morales la Madrid A, Cruz Martinez O, Hansford JR, Pietsch T et al. (2018) Molecularly defined diffuse leptomeningeal glioneuronal tumor (DLGNT) comprises two subgroups with distinct clinical and genetic features. Acta Neuropathol 136:239-253. doi:10.1007/s00401-018-1865-4

13.   Ellison DW, Hawkins C, Jones DTW, Onar-Thomas A, Pfister SM, Reifenberger G, Louis DN (2019) cIMPACT-NOW update 4: diffuse gliomas characterized by MYB, MYBL1, or FGFR1 alterations or BRAFV600E mutation. Acta Neuropathol:Online first. doi:10.1007/s00401-019-01987-0

14.   Gonda TJ, Buckmaster C, Ramsay RG (1989) Activation of c-myb by carboxy-terminal truncation: relationship to transformation of murine haemopoietic cells in vitro. The EMBO journal 8:1777-1783. doi:10.1002/j.1460-2075.1989.tb03571.x

15.   Gröbner SN, Worst BC, Weischenfeldt J, Buchhalter I, Kleinheinz K, Rudneva VA, Johann PD, Balasubramanian GP, Segura-Wang M, Brabetz S, Bender S, Hutter B, Sturm D, Pfaff E, Hübschmann D, Zipprich G, Heinold M, Eils J, Lawerenz C, Erkek S, Lambo S, Waszak S, Blattmann C, Borkhardt A, Kuhlen M et al. (2018) The landscape of genomic alterations across childhood cancers. Nature 555:321-327. doi:10.1038/nature25480

16.   Hansen KD, Aryee M (2012) IlluminaHumanMethylation450kmanifest: Annotation for Illumina's 450k methylation arrays. R package version 0.4.0. doi:10.18129/B9.bioc.IlluminaHumanMethylation450kmanifest

17.   Hansen KD, Aryee M (2016) IlluminaHumanMethylationEPICmanifest: Manifest for Illumina's EPIC methylation arrays. R package version 0.3.0. doi:10.18129/B9.bioc.IlluminaHumanMethylationEPICmanifest

18.   Hartmann C, Meyer J, Balss J, Capper D, Mueller W, Christians A, Felsberg J, Wolter M, Mawrin C, Wick W, Weller M, Herold-Mende C, Unterberg A, Jeuken JWM, Wesseling P, Reifenberger G, von Deimling A (2009) Type and frequency of IDH1 and IDH2 mutations are related to astrocytic and oligodendroglial differentiation and age: a study of 1,010 diffuse gliomas. Acta Neuropathol 118:469-474. doi:10.1007/s00401-009-0561-9

19.   Ho AS, Kannan K, Roy DM, Morris LGT, Ganly I, Katabi N, Ramaswami D, Walsh LA, Eng S, Huse JT, Zhang J, Dolgalev I, Huberman K, Heguy A, Viale A, Drobnjak M, Leversha MA, Rice CE, Singh B, Iyer NG, Leemans CR, Bloemena E, Ferris RL, Seethala RR, Gross BE et al. (2013) The mutational landscape of adenoid cystic carcinoma. Nat Genet 45:791-798. doi:10.1038/ng.2643

20.   Hou Y, Pinheiro J, Sahm F, Reuss DE, Schrimpf D, Stichel D, Casalini B, Koelsche C, Sievers P, Wefers AK, Reinhardt A, Ebrahimi A, Fernández-Klett F, Pusch S, Meier J, Schweizer L, Paulus W, Prinz M, Hartmann C, Plate KH, Reifenberger G, Pietsch T, Varlet P, Pagès M, Schüller U et al. (2019) Papillary glioneuronal tumor (PGNT) exhibits a characteristic methylation profile and fusions involving PRKCA. Acta Neuropathol. doi:10.1007/s00401-019-01969-2

21.   Hovestadt V, Remke M, Kool M, Pietsch T, Northcott P, Fischer R, Cavalli F, Ramaswamy V, Zapatka M, Reifenberger G, Rutkowski S, Schick M, Bewerunge-Hudler M, Korshunov A, Lichter P, Taylor M, Pfister S, Jones D (2013) Robust molecular subgrouping and copy-number profiling of medulloblastoma from small amounts of archival tumour material using high-density DNA methylation arrays. Acta Neuropathol 125:913-916. doi:10.1007/s00401-013-1126-5

22.   Hovestadt V, Zapatka M conumee: Enhanced copy-number variation analysis using Illumina DNA methylation arrays. R package version 1.9.0. doi:10.18129/B9.bioc.conumee

23.   Johann PD, Bens S, Oyen F, Wagener R, Giannini C, Perry A, Raisanen JM, Reis GF, Nobusawa S, Arita K, Felsberg J, Reifenberger G, Agaimy A, Buslei R, Capper D, Pfister SM, Schneppenheim R, Siebert R, Frühwald MC, Paulus W, Kool M, Hasselblatt M (2018) Sellar Region Atypical Teratoid/Rhabdoid Tumors (ATRT) in Adults Display DNA Methylation Profiles of the ATRT-MYC Subgroup. The American Journal of Surgical Pathology 42:506-511. doi:10.1097/PAS.0000000000001023

24.   Jones DTW, Hutter B, Jager N, Korshunov A, Kool M, Warnatz H-J, Zichner T, Lambert SR, Ryzhova M, Quang DAK, Fontebasso AM, Stutz AM, Hutter S, Zuckermann M, Sturm D, Gronych J, Lasitschka B, Schmidt S, Seker-Cin H, Witt H, Sultan M, Ralser M, Northcott PA, Hovestadt V, Bender S et al. (2013) Recurrent somatic alterations of FGFR1 and NTRK2 in pilocytic astrocytoma. Nat Genet 45:927-932. doi:10.1038/ng.2682

25. Jones DTW, Kieran MW, Bouffet E, Alexandrescu S, Bandopadhayay P, Bornhorst M, Ellison D, Fangusaro J, Fisher MI, Foreman N, Fouladi M, Hargrave D, Hawkins C, Jabado N, Massimino M, Mueller S, Perilongo G, van Meeteren AYNS, Tabori U, Warren K, Waanders AJ, Walker D, Weiss W, Witt O, Wright K et al. (2017) Pediatric low-grade gliomas: next biologically driven steps. Neuro Oncol 22:160-173. doi:10.1093/neuonc/nox141

26. Jones DTW, Kocialkowski S, Liu L, Pearson DM, Bäcklund LM, Ichimura K, Collins VP (2008) Tandem Duplication Producing a Novel Oncogenic BRAF Fusion Gene Defines the Majority of Pilocytic Astrocytomas. Cancer Res 68:8673. doi:10.1158/0008-5472.CAN-08-2097

27. Kanei-Ishii C, MacMillan EM, Nomura T, Sarai A, Ramsay RG, Aimoto S, Ishii S, Gonda TJ (1992) Transactivation and transformation by Myb are negatively regulated by a leucine-zipper structure. Proceedings of the National Academy of Sciences 89:3088-3092. doi:10.1073/pnas.89.7.3088

28. Koelsche C, Mynarek M, Schrimpf D, Bertero L, Serrano J, Sahm F, Reuss DE, Hou Y, Baumhoer D, Vokuhl C, Flucke U, Petersen I, Brück W, Rutkowski S, Zambrano SC, Garcia Leon JL, Diaz Coronado RY, Gessler M, Tirado OM, Mora J, Alonso J, Garcia del Muro X, Esteller M, Sturm D, Ecker J et al. (2018) Primary intracranial spindle cell sarcoma with rhabdomyosarcoma-like features share a highly distinct methylation profile and DICER1 mutations. Acta Neuropathol 136:327-337. doi:10.1007/s00401-018-1871-6

29. Li B, Dewey CN (2011) RSEM: accurate transcript quantification from RNA-Seq data with or without a reference genome. BMC Bioinformatics 12:323. doi:10.1186/1471-2105-12-323

30. Lin Y-C, Kuo M-W, Yu J, Kuo H-H, Lin R-J, Lo W-L, Yu AL (2008) c-Myb Is an Evolutionary Conserved miR-150 Target and miR-150/c-Myb Interaction Is Important for Embryonic Development. Mol Biol Evol 25:2189-2198. doi:10.1093/molbev/msn165

31. Liu Y, Easton J, Shao Y, Maciaszek J, Wang Z, Wilkinson MR, McCastlain K, Edmonson M, Pounds SB, Shi L, Zhou X, Ma X, Sioson E, Li Y, Rusch M, Gupta P, Pei D, Cheng C, Smith MA, Auvil JG, Gerhard DS, Relling MV, Winick NJ, Carroll AJ, Heerema NA et al. (2017) The genomic landscape of pediatric and young adult T-lineage acute lymphoblastic leukemia. Nat Genet 49:1211-1218. doi:10.1038/ng.3909

32. Louis DN, Ohgaki H, Wiestler OD, Cavenee WK (2016) WHO Classification of Tumours of the Central Nervous System. Revised 4th edition edn. IARC, Lyon

33. Oh IH, Reddy EP (1999) The myb gene family in cell growth, differentiation and apoptosis. Oncogene 18:3017-3033. doi:10.1038/sj.onc.1202839

34. Pajtler KW, Wen J, Sill M, Lin T, Orisme W, Tang B, Hübner J-M, Ramaswamy V, Jia S, Dalton JD, Haupfear K, Rogers HA, Punchihewa C, Lee R, Easton J, Wu G, Ritzmann TA, Chapman R, Chavez L, Boop FA, Klimo P, Sabin ND, Ogg R, Mack SC, Freibaum BD et al. (2018) Molecular heterogeneity and CXorf67 alterations in posterior fossa group A (PFA) ependymomas. Acta Neuropathol. doi:10.1007/s00401-018-1877-0

35. Pajtler KW, Witt H, Sill M, Jones DTW, Hovestadt V, Kratochwil F, Wani K, Tatevossian R, Punchihewa C, Johann P, Reimand J, Warnatz H-J, Ryzhova M, Mack S, Ramaswamy V, Capper D, Schweizer L, Sieber L, Wittmann A, Huang Z, van Sluis P, Volckmann R, Koster J, Versteeg R, Fults D et al. (2015) Molecular Classification of Ependymal Tumors across All CNS Compartments, Histopathological Grades, and Age Groups. Cancer Cell 27:728-743. doi:10.1016/j.ccell.2015.04.002

36. Persson M, Andrén Y, Mark J, Horlings HM, Persson F, Stenman G (2009) Recurrent fusion of MYB and NFIB transcription factor genes in carcinomas of the breast and head and neck. Proceedings of the National Academy of Sciences 106:18740-18744. doi:10.1073/pnas.0909114106

37. Qaddoumi I, Orisme W, Wen J, Santiago T, Gupta K, Dalton JD, Tang B, Haupfear K, Punchihewa C, Easton J, Mulder H, Boggs K, Shao Y, Rusch M, Becksfort J, Gupta P, Wang S, Lee RP, Brat D, Peter Collins V, Dahiya S, George D, Konomos W, Kurian KM, McFadden K et al. (2016) Genetic alterations in uncommon low-grade neuroepithelial tumors: BRAF, FGFR1, and MYB mutations occur at high frequency and align with morphology. Acta Neuropathol:1-13. doi:10.1007/s00401-016-1539-z

38.   Quelen C, Lippert E, Struski S, Demur C, Soler G, Prade N, Delabesse E, Broccardo C, Dastugue N, Mahon F-X, Brousset P (2011) Identification of a transforming MYB-GATA1 fusion gene in acute basophilic leukemia: a new entity in male infants. Blood 117:5719-5722. doi:10.1182/blood-2011-01-333013

39.   Ramkissoon LA, Horowitz PM, Craig JM, Ramkissoon SH, Rich BE, Schumacher SE, McKenna A, Lawrence MS, Bergthold G, Brastianos PK, Tabak B, Ducar MD, Van Hummelen P, MacConaill LE, Pouissant-Young T, Cho Y-J, Taha H, Mahmoud M, Bowers DC, Margraf L, Tabori U, Hawkins C, Packer RJ, Hill DA, Pomeroy SL et al. (2013) Genomic analysis of diffuse pediatric low-grade gliomas identifies recurrent oncogenic truncating rearrangements in the transcription factor MYBL1. Proceedings of the National Academy of Sciences 110:8188-8193. doi:10.1073/pnas.1300252110

40.   Ramsay RG, Gonda TJ (2008) MYB function in normal and cancer cells. Nat Rev Cancer 8:523-534. doi:10.1038/nrc2439

41.   Reinhardt A, Stichel D, Schrimpf D, Sahm F, Korshunov A, Reuss DE, Koelsche C, Huang K, Wefers AK, Hovestadt V, Sill M, Gramatzki D, Felsberg J, Reifenberger G, Koch A, Thomale U-W, Becker A, Hans VH, Prinz M, Staszewski O, Acker T, Dohmen H, Hartmann C, Mueller W, Tuffaha MSA et al. (2018) Anaplastic astrocytoma with piloid features, a novel molecular class of IDH wildtype glioma with recurrent MAPK pathway, CDKN2A/B and ATRX alterations. Acta Neuropathol 136:273-291. doi:10.1007/s00401-018-1837-8

42.   Reuss DE, Kratz A, Sahm F, Capper D, Schrimpf D, Koelsche C, Hovestadt V, Bewerunge-Hudler M, Jones DW, Schittenhelm J, Mittelbronn M, Rushing E, Simon M, Westphal M, Unterberg A, Platten M, Paulus W, Reifenberger G, Tonn J-C, Aldape K, Pfister S, Korshunov A, Weller M, Herold-Mende C, Wick W et al. (2015) Adult IDH wild type astrocytomas biologically and clinically resolve into other tumor entities. Acta Neuropathol 130:407-417. doi:10.1007/s00401-015-1454-8

43.   Robinson JT, Thorvaldsdóttir H, Winckler W, Guttman M, Lander ES, Getz G, Mesirov JP (2011) Integrative genomics viewer. Nat Biotechnol 29:24-26. doi:10.1038/nbt.1754

44.   Sahm F, Reuss D, Koelsche C, Capper D, Schittenhelm J, Heim S, Jones DTW, Pfister SM, Herold-Mende C, Wick W, Mueller W, Hartmann C, Paulus W, von Deimling A (2014) Farewell to oligoastrocytoma: in situ molecular genetics favor classification as either oligodendroglioma or astrocytoma. Acta Neuropathol 128:551-559. doi:10.1007/s00401-014-1326-7

45.   Sahm F, Schrimpf D, Stichel D, Jones DTW, Hielscher T, Schefzyk S, Okonechnikov K, Koelsche C, Reuss DE, Capper D, Sturm D, Wirsching H-G, Berghoff AS, Baumgarten P, Kratz A, Huang K, Wefers AK, Hovestadt V, Sill M, Ellis HP, Kurian KM, Okuducu AF, Jungk C, Drueschler K, Schick M et al. (2017) DNA methylation-based classification and grading system for meningioma: a multicentre, retrospective analysis. The Lancet Oncology 18:682-694. doi:10.1016/S1470-2045(17)30155-9

46.   Schindler G, Capper D, Meyer J, Janzarik W, Omran H, Herold-Mende C, Schmieder K, Wesseling P, Mawrin C, Hasselblatt M, Louis DN, Korshunov A, Pfister S, Hartmann C, Paulus W, Reifenberger G, von Deimling A (2011) Analysis of BRAF V600E mutation in 1,320 nervous system tumors reveals high mutation frequencies in pleomorphic xanthoastrocytoma, ganglioglioma and extra-cerebellar pilocytic astrocytoma. Acta Neuropathol 121:397-405. doi:10.1007/s00401-011-0802-6

47.   Schramm J, Luyken C, Urbach H, Fimmers R, Blumcke I (2004) Evidence for a clinically distinct new subtype of grade II astrocytomas in patients with long-term epilepsy. Neurosurgery 55:340-347. doi:10.1227/01.NEU.0000129546.38675.1B

48.   Sievers P, Stichel D, Schrimpf D, Sahm F, Koelsche C, Reuss DE, Wefers AK, Reinhardt A, Huang K, Ebrahimi A, Hou Y, Pajtler KW, Pfister SM, Hasselblatt M, Stummer W, Schick U, Hartmann C, Hagel C, Staszewski O, Reifenberger G, Beschorner R, Coras R, Keyvani K, Kohlhof P, Diomedi-Camassei F et al. (2018) FGFR1:TACC1 fusion is a frequent event in molecularly defined extraventricular neurocytoma. Acta Neuropathol 136:293-302. doi:10.1007/s00401-018-1882-3

49.   Stichel D, Schrimpf D, Casalini B, Meyer J, Wefers AK, Sievers P, Korshunov A, Koelsche C, Reuss DE, Reinhardt A, Ebrahimi A, Fernandéz-Klett F, Kessler T, Sturm D, Ecker J, Milde T, Herold-Mende C, Witt O, Pfister SM, Wick W, Jones DTW, von Deimling A, Sahm F (2019) Routine RNA sequencing from formalin-fixed paraffin-embedded specimens in neuropathology diagnostics identifies diagnostically and therapeutically relevant gene fusions. Acta Neuropathol (accepted for publication)

50.   Sturm D, Orr BA, Toprak UH, Hovestadt V, Jones DTW, Capper D, Sill M, Buchhalter I, Northcott PA, Leis I, Ryzhova M, Koelsche C, Pfaff E, Allen SJ, Balasubramanian G, Worst BC, Pajtler KW, Brabetz S, Johann PD, Sahm F, Reimand J, Mackay A, Carvalho DM, Remke M, Phillips JJ et al. (2016) New Brain Tumor Entities Emerge from Molecular Classification of CNS-PNETs. Cell 164:1060-1072. doi:10.1016/j.cell.2016.01.015

51.   Sturm D, Witt H, Hovestadt V, Khuong-Quang DA, Jones DT, Konermann C, Pfaff E, Tönjes M, Sill M, Bender S, Kool M, Zapatka M, Becker N, Zucknick M, Hielscher T, Liu XY, Fontebasso AM, Ryzhova M, Albrecht S, Jacob K, Wolter M, Ebinger M, Schuhmann MU, van Meter T, Frühwald MC et al. (2012) Hotspot Mutations in H3F3A and IDH1 Define Distinct Epigenetic and Biological Subgroups of Glioblastoma. Cancer Cell 22:425-437. doi:10.1016/j.ccr.2012.08.024

52.   Suzuki K, Suzuki Y, Hama A, Muramatsu H, Nakatochi M, Gunji M, Ichikawa D, Hamada M, Taniguchi R, Kataoka S, Murakami N, Kojima D, Sekiya Y, Nishikawa E, Kawashima N, Narita A, Nishio N, Nakazawa Y, Iwafuchi H, Watanabe Ki, Takahashi Y, Ito M, Kojima S, Kato S, Okuno Y (2017) Recurrent MYB rearrangement in blastic plasmacytoid dendritic cell neoplasm. Leukemia 31:1629-1633. doi:10.1038/leu.2017.101

53.   Takahashi T, Nakagoshi H, Sarai A, Nomura N, Yamamoto T, Ishii S (1995) Human A-myb gene encodes a transcriptional activator containing the negative regulatory domains. FEBS Lett 358:89-96. doi:10.1016/0014-5793(94)01402-M

54.   Tatevossian R, Tang B, Dalton J, Forshew T, Lawson A, Ma J, Neale G, Shurtleff S, Bailey S, Gajjar A, Baker S, Sheer D, Ellison D (2010) MYB upregulation and genetic aberrations in a subset of pediatric low-grade gliomas. Acta Neuropathol 120:731-743. doi:10.1007/s00401-010-0763-1

55.   Urbach H, Binder D, von Lehe M, Podlogar M, Bien CG, Becker A, Schramm J, Kral T, Clusmann H (2007) Correlation of MRI and histopathology in epileptogenic parietal and occipital lobe lesions. Seizure 16:608-614. doi:10.1016/j.seizure.2007.04.009

56.   Weston K (1998) Myb proteins in life, death and differentiation. Curr Opin Genet Dev 8:76-81. doi:10.1016/S0959-437X(98)80065-8

57.   Xiao C, Calado DP, Galler G, Thai T-H, Patterson HC, Wang J, Rajewsky N, Bender TP, Rajewsky K (2007) MiR-150 Controls B Cell Differentiation by Targeting the Transcription Factor c-Myb. Cell 131:146-159. doi:10.1016/j.cell.2007.07.021

58.   Yan H, Parsons DW, Jin G, McLendon R, Rasheed BA, Yuan W, Kos I, Batinic-Haberle I, Jones S, Riggins GJ, Friedman H, Friedman A, Reardon D, Herndon J, Kinzler KW, Velculescu VE, Vogelstein B, Bigner DD (2009) IDH1 and IDH2 Mutations in Gliomas. New Engl J Med 360:765-773. doi:10.1056/NEJMoa0808710

59.   Zhang J, Wu G, Miller CP, Tatevossian RG, Dalton JD, Tang B, Orisme W, Punchihewa C, Parker M, Qaddoumi I, Boop FA, Lu C, Kandoth C, Ding L, Lee R, Huether R, Chen X, Hedlund E, Nagahawatte P, Rusch M, Boggs K, Cheng J, Becksfort J, Ma J, Song G et al. (2013) Whole-genome sequencing identifies genetic alterations in pediatric low-grade gliomas. Nat Genet 45:602-612. doi:10.1038/ng.2611

60.   Zhao H, Kalota A, Jin S, Gewirtz AM (2009) The c-myb proto-oncogene and microRNA-15a comprise an active autoregulatory feedback loop in human hematopoietic cells. Blood 113:505. doi:10.1182/blood-2008-01-136218

Figure captions

Fig. 1 Isomorphic diffuse gliomas are monomorphic, IDH-wildtype tumours with low proliferation. **a–d** Histologically typical isomorphic diffuse gliomas showing round, only minimally pleomorphic nuclei, often with speckled chromatin. The cell density is slightly (**a, d**) to moderately (**b, c**) increased. The fibrillary matrix between the tumour cells can have slight (**c**) to extensive (**d**) microcystic changes. In some tumours scattered pre-existing neurons (arrows in **b, e, f**) are observed. **e** Occasionally, isomorphic diffuse gliomas may have smaller, more condensed round nuclei resembling those of oligodendrocytes. **f** One case focally showed myxoid changes of the matrix with scattered residual neurons, resembling the glio-neuronal element of dysembryoplastic neuroepithelial tumours. In other areas, the tumour also showed a clearly isomorphic growth. **g–l** Immunohistochemically, isomorphic diffuse gliomas are GFAP-positive (**g**; same tumour as in **a**) whereas MAP2 only labels residual neurons and neuronal processes (**h**). The tumours are CD34-negative (**i**) and IDH1 R132H-negative (**j**) with a retained nuclear expression of ATRX (**k**). The Ki67 proliferation index is below 1% (**l**). Scale bars 200 µm in **a** for **a–l**, 25 µm in the inset in **a** for all insets in **a–f**

Fig. 2 Isomorphic diffuse glioma forms a distinct methylation cluster. **a** Unsupervised hierarchical cluster analysis of 26 isomorphic diffuse gliomas with 246 cases from 17 reference classes. **b** t-distributed stochastic neighbor embedding (t-SNE) analysis of the same cases. Isomorphic diffuse glioma forms a cluster distinct from other glial/glio-neuronal tumour entities and normal cortex and white matter. The closest relation was found to the cluster of angiocentric glioma.

Fig. 3 A subset of isomorphic diffuse gliomas has copy number alterations of the *MYBL1-* and *MYB*-genes. **a–d** Exemplary copy number profiles (CNP) of isomorphic diffuse gliomas. Gains are shown in green, losses in red. (**a**) Gain from *MYBL1* to *MMP16* (# 2; similar CNP in # 1). (**b**) Loss from *MYBL1* to *TOX* (# 5). (**c**) Gain of *MYB* plus gain of *HMG20A* on chromosome 15 (# 15). (**d**) Loss of *MYB* and the region 3' of *MYB* (# 17).

Fig. 4 Isomorphic diffuse gliomas have fusions of the *MYBL1*- and *MYB*-genes and show a corresponding mRNA-overexpression. **a, b** Canonical MYBL1- (**a**) and MYB-protein (**b**) with loci of fusions to different partners. Protein domains in blue: "SANT" DNA-binding domain, "LMSTEN" transactivating domain, "C-myb" C-terminal negative regulatory domain. Fusions result in a deletion of the C-terminal negative regulatory C-myb domain of MYBL1 (**a**) or MYB (**b**), or the 3' miRNA-binding sites of *MYB* (not included in depiction as no part of the MYB protein). (**c, d**) Many isomorphic diffuse gliomas show an overexpression of *MYBL1* (**c**) or *MYB* (**d**). Compared were pilocytic astrocytomas ("PA"), isomorphic diffuse gliomas with *MYBL1* alterations ("*MYBL1* IDG") or *MYB* alterations ("*MYB* IDG") in the CNP and/or RNA sequencing, and isomorphic diffuse gliomas without evidence of *MYBL1/MYB* alterations ("other IDG"). Outliers are depicted with filled circles. p = 0.022 for PA versus *MYBL1* IDG in **c**, p = 0.009 for *MYBL1* versus *MYB* IDG in **d** (p-values adjusted for multiple comparisons). (**e**) Summary of alterations of *MYBL1* and *MYB* in the 26 isomorphic diffuse gliomas of this study detected with different methods. For better differentiation, the range of the colour scale for the *MYBL1* expression does not account for the outlier. #: case number

Fig. 5 Patients with isomorphic diffuse gliomas have a good prognosis. Kaplan-Meier-analysis showing overall survival of patients with isomorphic diffuse gliomas (IDG), angiocentric gliomas WHO grade I (AG), pilocytic astrocytomas WHO grade I (PA) and diffuse astrocytomas, IDH-mutant, WHO grade II (AII, IDH-mutant). Note that no patient with IDG died during follow-up.

Figure 1
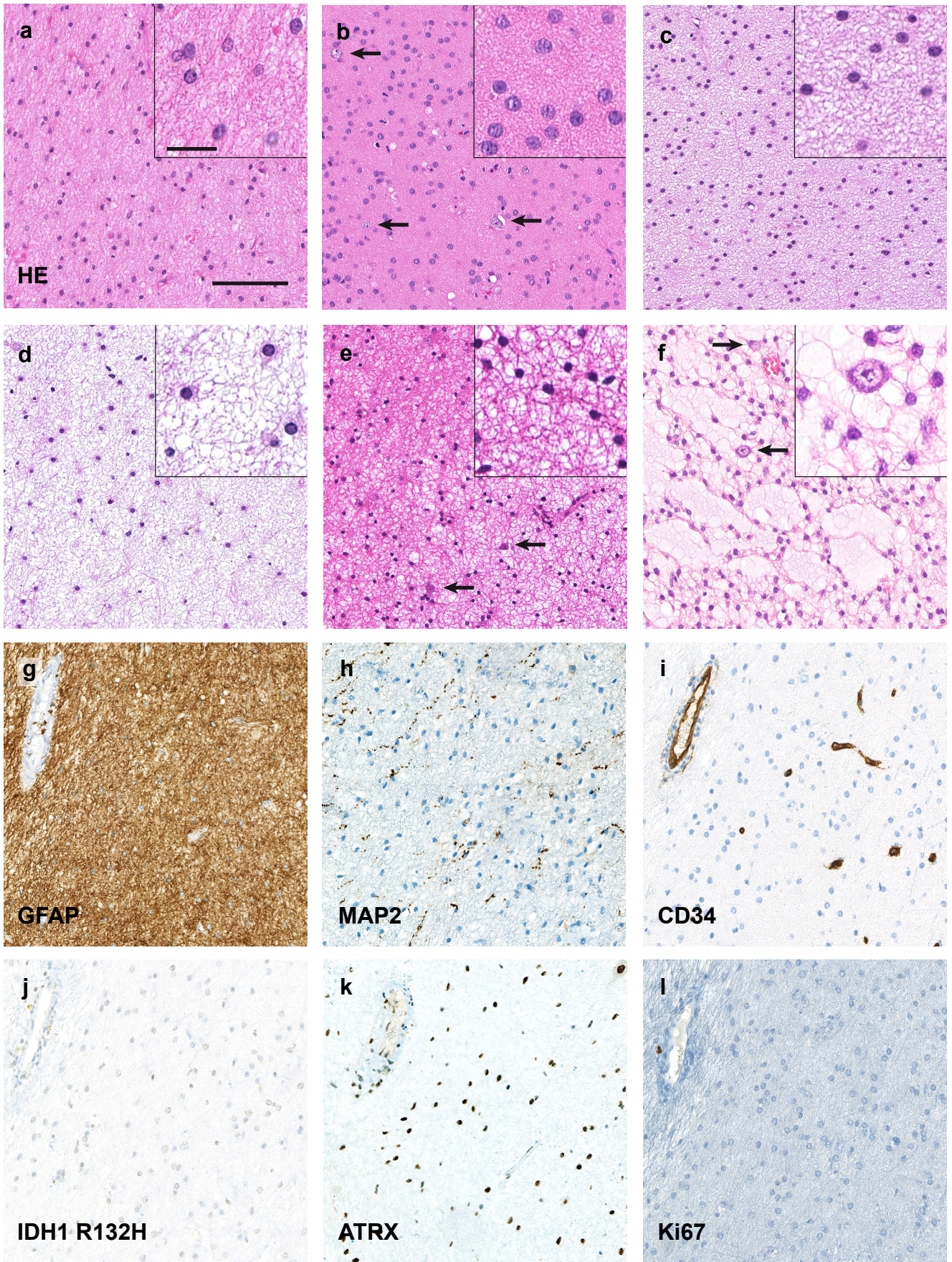
Figure 2
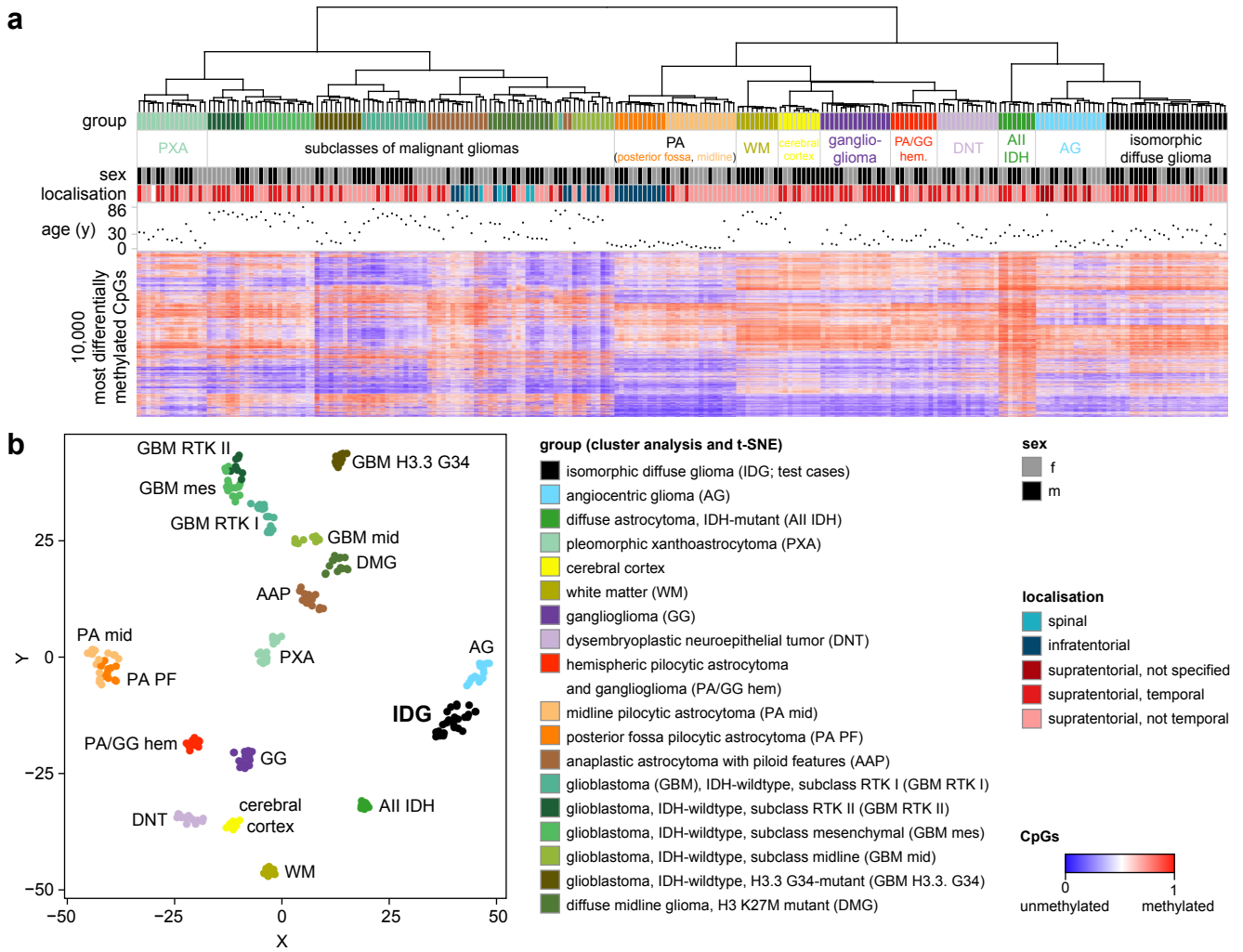
Figure 3
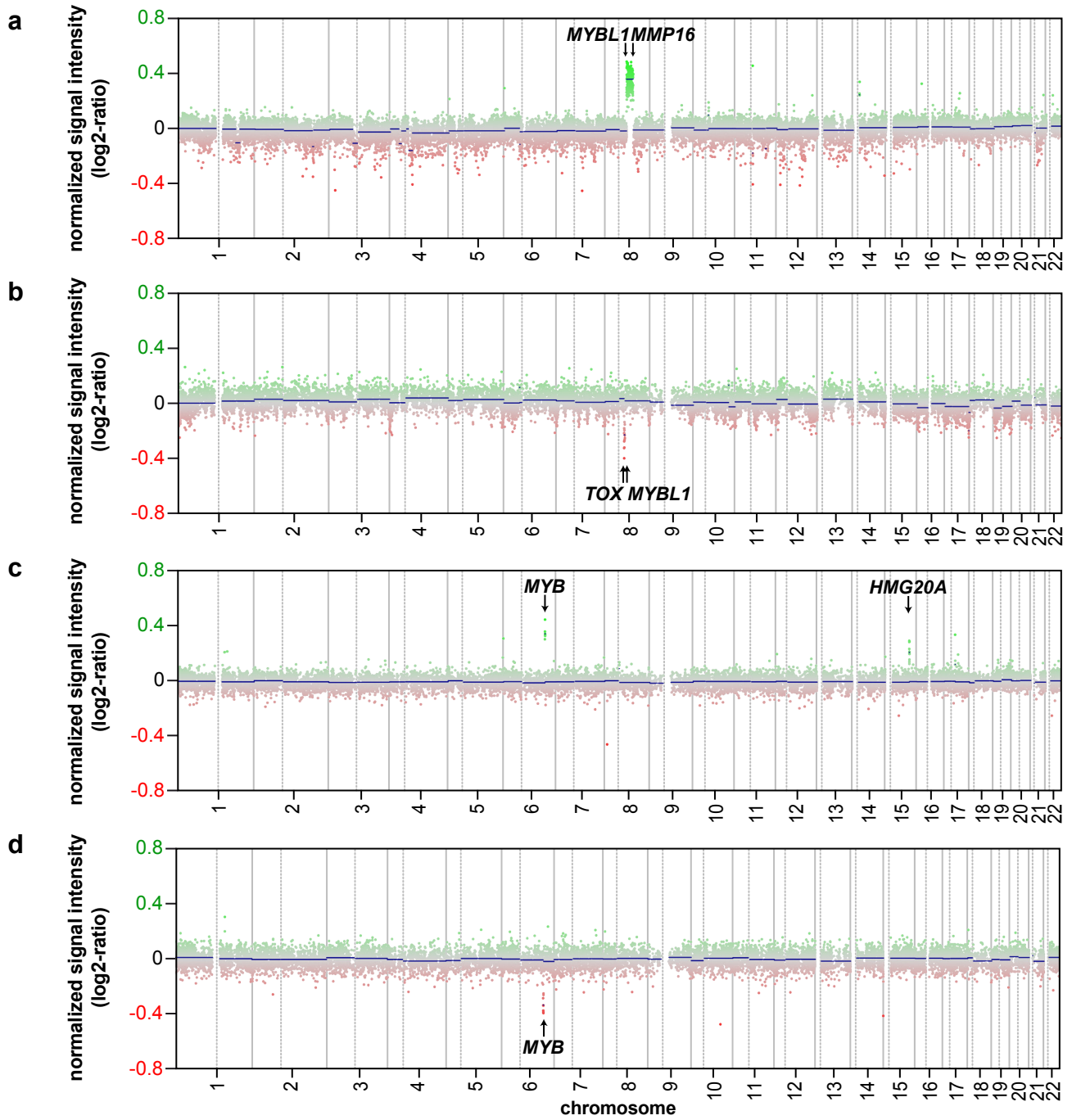
Figure 4

a MYBL1 fusions

b MYB fusions

c

d

e
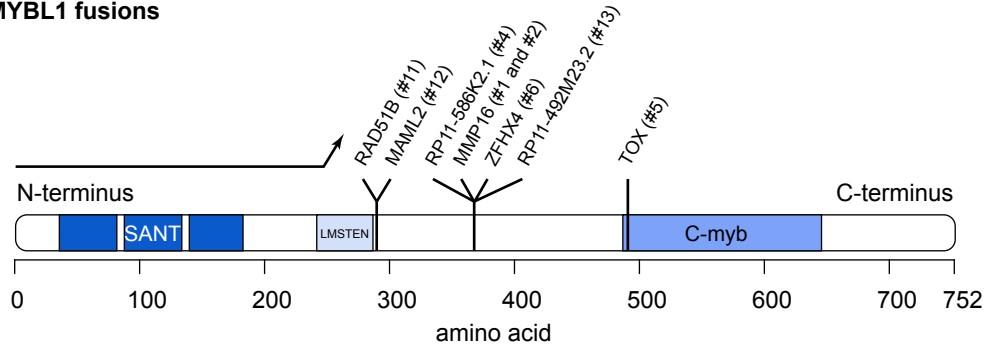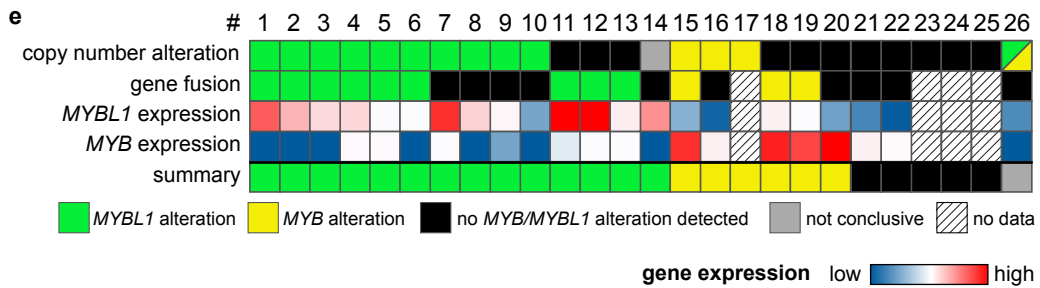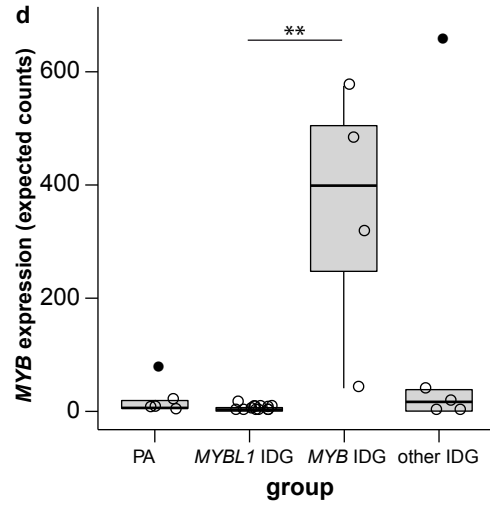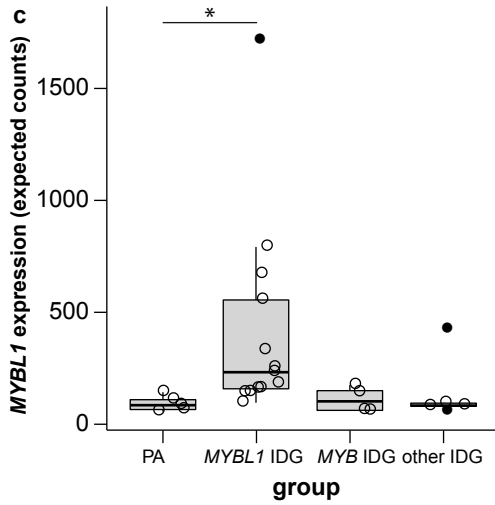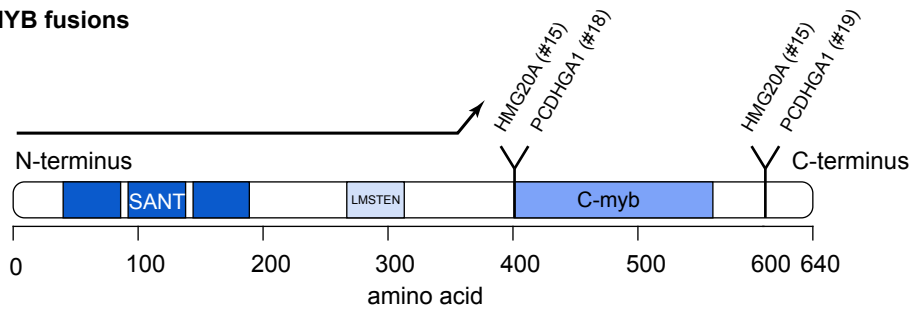
Figure 5
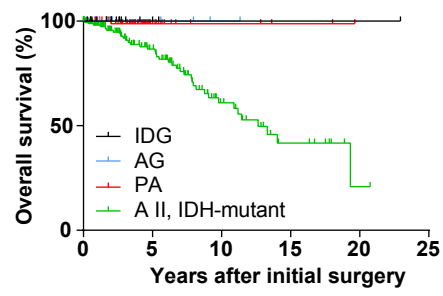
Number at risk

IDG	18	3	1	1	1
AG	10	4	1	0	0
PA	82	18	4	2	0
A II, IDH-mutant	181	73	24	9	1
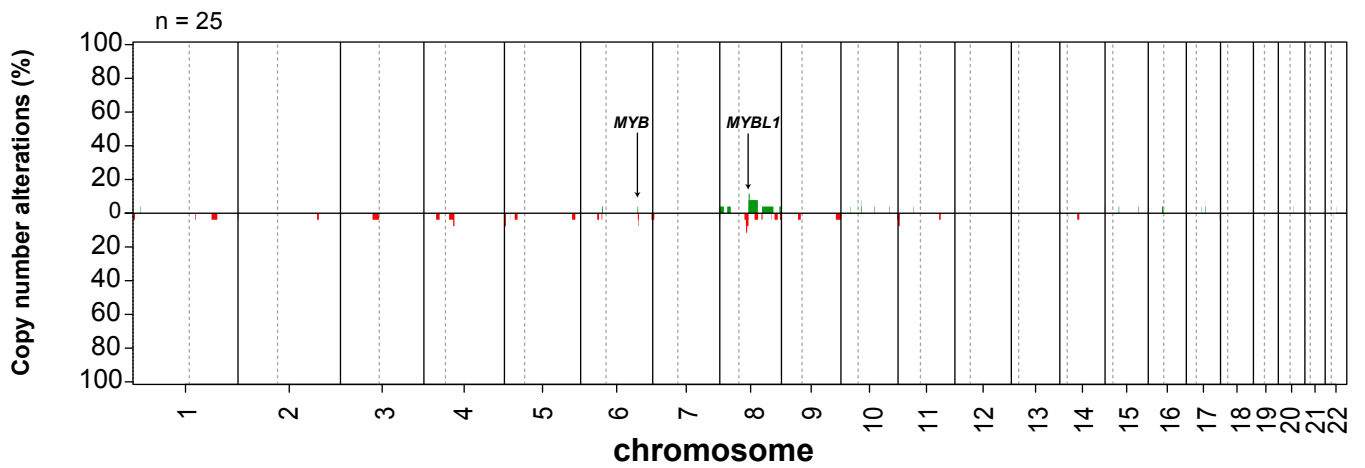
Supplementary Fig. 1 Summary copy number profile of isomorphic diffuse glioma.
The percentages are based on the copy number profiles of all 25 isomorphic diffuse gliomas with high quality copy number profiles
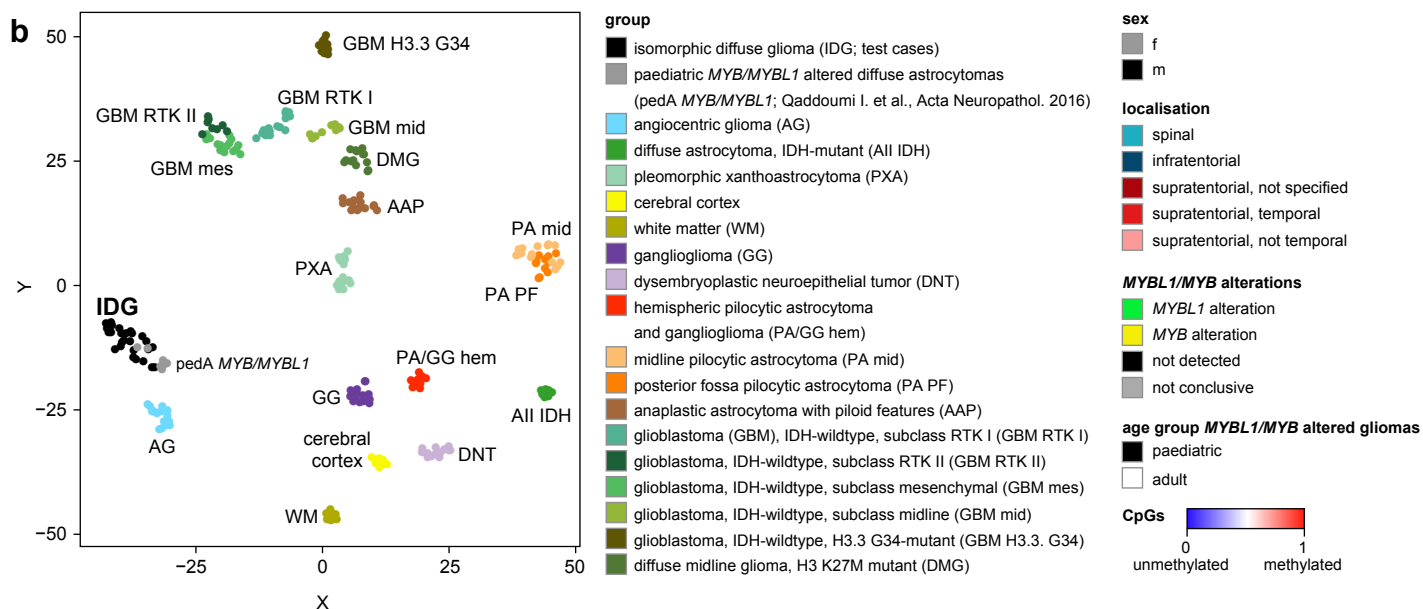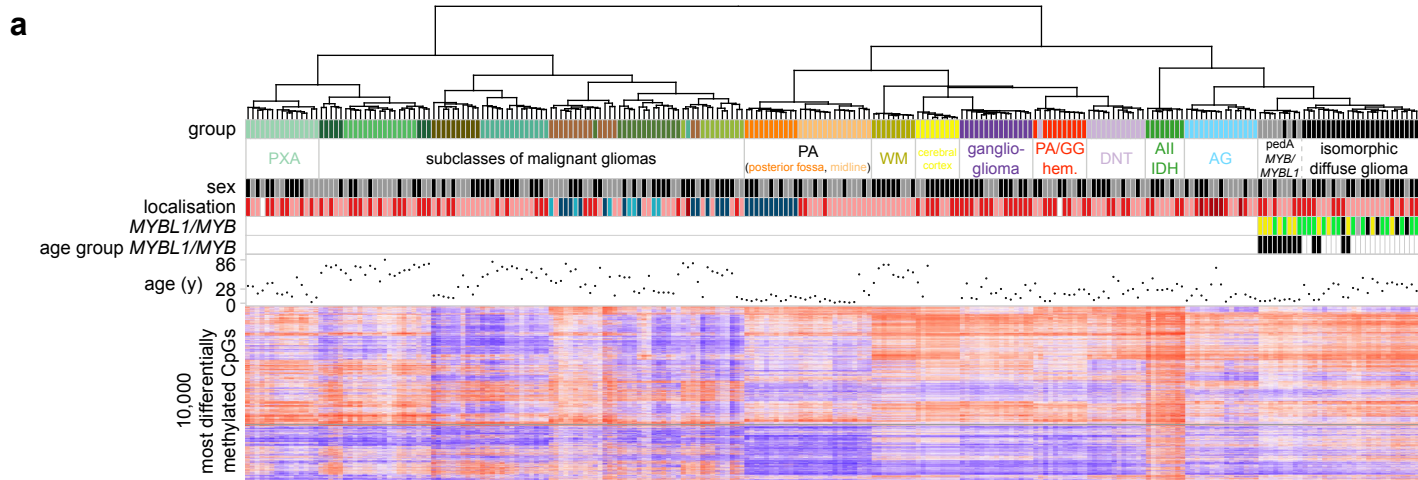
Supplementary Fig. 2 Isomorphic diffuse glioma forms a distinct methylation cluster related to paediatric *MYB/MYBL1* altered diffuse astrocytomas and angiocentric gliomas.

a Unsupervised hierarchical cluster analysis of the cases from Fig. 2 in conjunction with published methylation data from seven paediatric *MYB/MYBL1* altered diffuse astrocytomas (Qaddoumi I. et al., Acta Neuropathol. 2016). All seven paediatric *MYB/MYBL1* altered diffuse astrocytomas cluster together. In addition, two isomorphic diffuse gliomas fall into the same cluster while the other isomorphic diffuse gliomas form a separate cluster. **b** t-distributed stochastic neighbor embedding (t-SNE) analysis of the same cases. Again, paediatric *MYB/MYBL1* altered diffuse astrocytomas mostly separate from isomorphic diffuse glioma with the identical two isomorphic diffuse gliomas as in (**a**) falling in close proximity. In addition, two paediatric *MYB/MYBL1* altered diffuse astrocytomas intermingle with the neighbouring isomorphic diffuse gliomas, indicating a close relation or even partial overlap of these two groups